The American Journal of Engineering and Technology
ISSN 2689-0984 Volume 08 - 2026

Features Of Geomechanical Processes Of Subcritical Deformation In The Vicinity Of The Face And Intersections Of Underground Mine Openings

[1] Buriyev Shukurulla Ubaydullayevich
[1] Nazarov Zair Sadikovich
[1] Jiyanov Abdunor Bobokulovich
[1] Avazov Adxambek Nurilla o‘g‘li

[1] Navoi State Mining and Technologies University, Uzbekistan

Received: 29th Dec 2025 | Received Revised Version: 15th Jan 2026 | Accepted: 28th Jan 2026 | Published: 16th Feb 2026
Volume 08 Issue 02 2026 | Crossref DOI: 10.37547/tajet/Volume08Issue02-11

Abstract

This paper investigates the geomechanical behavior of rock masses in the zone of subcritical deformation around underground mine openings. The relationship between deformation and failure processes is analyzed with emphasis on stress–strain interaction under varying structural, geometric, and stress conditions. Analytical models were used to evaluate the distribution of stresses and displacements in homogeneous, isotropic, linearly deformable rock masses surrounding circular and non-circular excavations under different lateral pressure coefficients. The results demonstrate that maximum tangential stress occurs along zones of maximum curvature in the excavation contour, while stress concentration diminishes rapidly with distance from the excavation boundary. It is shown that subcritical deformation analysis allows prediction of post-critical rock pressure phenomena and provides a reliable basis for assessing the stability of underground workings. The presence of technological heterogeneities of blasting origin slightly increases displacements but reduces the influence of anisotropic stress conditions and contour shape, simplifying analytical modeling of the rock mass.

Keywords: Subcritical deformation; rock mass; stress–strain state; underground excavation; lateral pressure coefficient; tangential stress concentration; geomechanics; mining engineering; isotropic model; excavation stability.

Cite This Article: Buriyev Shukurulla Ubaydullayevich, Nazarov Zair Sadikovich, Jiyanov Abdunor Bobokulovich, & Avazov Adxambek Nurilla o‘g‘li. (2026). Features Of Geomechanical Processes Of Subcritical Deformation In The Vicinity Of The Face And Intersections Of Underground Mine Openings. The American Journal of Engineering and Technology, 8(2), 118–125. https://doi.org/10.37547/tajet/Volume08Issue02-11

1. Introduction

The distinction between deformation and failure processes in rock masses is conditional. Rock destruction begins during the subcritical deformation stage and manifests fully at the post-critical stage, largely determining the magnitude of observed displacements. As deformation increases beyond the strength limit, the load-bearing capacity of the rock mass decreases. Thus, deformation and failure processes are organically interconnected, mutually influencing and quantitatively determining each other [1].

At the subcritical stage, as deformation grows, stresses increase up to a limiting level; upon unloading, most of the deformation is recovered, and rock loosening is minimal. The study of subcritical deformation, when failure has not yet developed, is more accessible for researchers and enables assessment of the main factors determining the mechanical behavior of the rock mass prior to failure. Consequently, analyzing these factors allows a degree of prediction of post-critical deformation patterns and the manifestation of rock pressure phenomena.

The distinction between deformation and failure processes in rock masses is conditional. The process of rock failure begins at the subcritical deformation stage and is fully manifested at the post-critical stage, practically determining the magnitude of the observed deformations. On the other hand, as deformation increases beyond the strength limit, the load-bearing capacity of the rock mass decreases. Thus, the deformation and failure processes are organically interconnected; they mutually penetrate each other and quantitatively define one another [2].

At the subcritical stage, as deformation increases, the stresses grow up to a limiting level. During unloading, most of the deformation is recovered, and rock loosening remains insignificant. It should be noted that studying subcritical deformation of rock masses, when failure processes have not yet developed, is more accessible for researchers. In this sense, it allows for evaluating the influence of most factors that determine the mechanical state of the rock mass during the subcritical deformation stage. Consequently, analyzing the factors influencing subcritical deformation makes it possible, to a certain extent, to predict the patterns of post-critical deformation and the manifestation of rock pressure.

Hence, the main objective in studying subcritical deformation is to perform a qualitative and quantitative analysis of its regularities under the influence of various factors. The most significant of these factors include:

Structural and mechanical characteristics of the rock mass (physical and geometrical anisotropy, artificial heterogeneity, and initial stress state);

Type of excavation (drift, chamber, or stope), the shape of its cross-section, and the influence of the excavation face;

Behavioral laws of rocks under load (nonlinear deformation, rheological processes, etc.).

2. Methods

In this study, the stress–strain state resulting from subcritical deformation of rock masses around underground excavations is analyzed, taking into account the above-mentioned factors. This analysis can be performed analytically, without the use of numerical methods. The investigation begins with solving the simplest case, where the rock mass can be represented by a homogeneous, isotropic, linearly deformable geomechanical model [3]. The initial stress field is considered equiaxial, and the excavation is assumed to have a circular cross-section and to be elongated and deep-seated. The solution to this basic case is taken as a reference, against which the influence of various factors on the stress–strain state of the rock mass will be evaluated.

When studying geomechanical processes in the vicinity of horizontal, deep-seated, elongated openings with circular cross-sections, excavated in a homogeneous, isotropic, and “incompressible” rock mass (with Poisson’s ratio equal to 0.5) under an equiaxial initial stress field, one can employ the axisymmetric solution of elasticity theory. If the axis of the cylindrical coordinate system coincides with the longitudinal axis of the excavation, the rock mass sections normal to the axis will be in a plane strain state. In other words, in this case, the problem can be considered in the formulation of plane strain with axial symmetry [4].

$$\sigma_z = \sigma_r = \sigma_\theta = q\ ,\ \tau_{rz} = \tau_{r\theta} = \tau_{\theta z} = 0, \qquad (1)$$

where q accounts for the influence of gravitational forces and other contributing factors.

The corresponding analytical scheme for determining the additional stresses in the rock mass is shown in Figure 1.

In this case, the boundary conditions are expressed as follows:

$\sigma_r = p - q$ at $r = 1$ (along the excavation contour),

$$\sigma_r = \sigma_\theta \to 0 \quad \text{at} \quad r = \infty \qquad (2)$$

where p is the support (lining) reactive pressure.

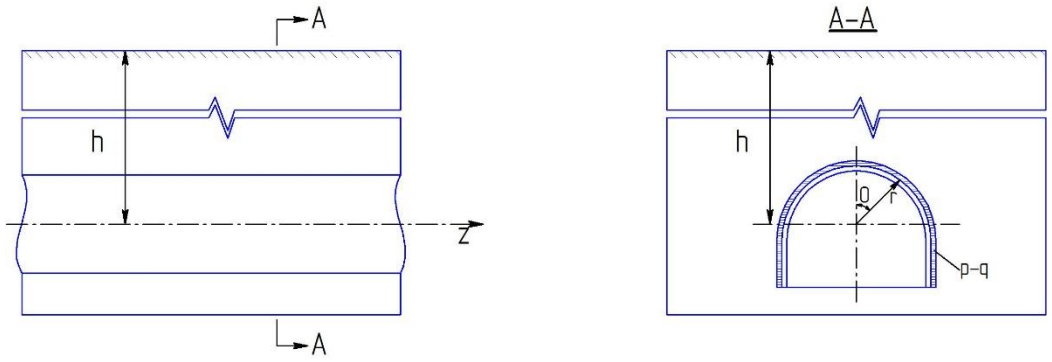

Fig. 1. Calculation scheme of the rock mass surrounding a horizontal excavation for determining additional stresses.

The components of the additional stresses, obtained from the solution of the problem, are expressed as follows [5]:

$$\sigma_r = \frac{p-q}{r^2}, \quad \sigma_\theta = \frac{p-q}{r^2}, \quad \sigma_z = \frac{p-q}{r^2}, \quad \sigma_z = 0, \ \tau_{rz} = \tau_{r\theta} = \tau_{\theta z} = 0. \tag{3}$$

The total stresses in the rock mass are determined by summing the initial stresses (1) and the additional stresses (3):

$$\sigma_r = q + \frac{p-q}{r^2}, \quad \sigma_\theta = q - \frac{p-q}{r^2},$$

$$\sigma_z = q, \ \tau_{rz} = \tau_{r\theta} = \tau_{\theta z} = 0. \tag{4}$$

The components of deformation, which by their nature are additional, are determined using the additional stress components (3):

$$\varepsilon_\theta = -\varepsilon_r = \frac{3}{2E}\frac{q-p}{r^2}. \tag{5}$$

Corresponding radial dimensionless displacements [6]

$$u = r\varepsilon_\theta = \frac{3}{2E}\frac{q-p}{r}. \tag{6}$$

The analysis of the distribution patterns of the total stresses σ_r and σ_θ around the excavation shows that along its boundary at $r = 1$ the tangential stress σ_θ reaches its maximum value, while the radial stress σ_r is minimal. As the distance from the excavation boundary increases, the stresses gradually approach the initial stresses in the undisturbed rock mass.

Table 1 presents the values of σ_r ,σ_θ , and σ_z for $p = 0$ (an unsupported excavation). It is clearly seen that, in this case, the stress concentration factor** along the boundary of a circular excavation is equal to two and does not depend on the location of the considered point along the boundary. Displacements also reach their

maximum at the excavation boundary and rapidly decay with increasing distance into the rock mass.

Table 1.

r	**Stresses are given in units of *q***			*r*	**Stresses are given in units of *q***		
	σ_r	σ_θ	σ_z		σ_r	σ_θ	σ_z
1	0	2,00	1,0	6	0,97	1,03	1,0
2	0,75	1,25	1,0	10	0,99	1,01	1,0
3	0,94	1,06	1,0				

If the initial stress state of the rock mass differs from a hydrostatic (equal-component) state, the conditions of symmetry are violated. Let us consider an initial stress state of the rock mass with equal horizontal stress components (M), which, in a rectangular coordinate system, can be represented as [7]:

$$\sigma_y = q, \sigma_z = \sigma_x = \lambda q, \qquad \tau_{xy} = \tau_{xz} = \tau_{yz} = 0, \quad (7)$$

Transitioning to cylindrical coordinates, let us assume that the angle θ is measured from the vertical axis (Fig. 2).

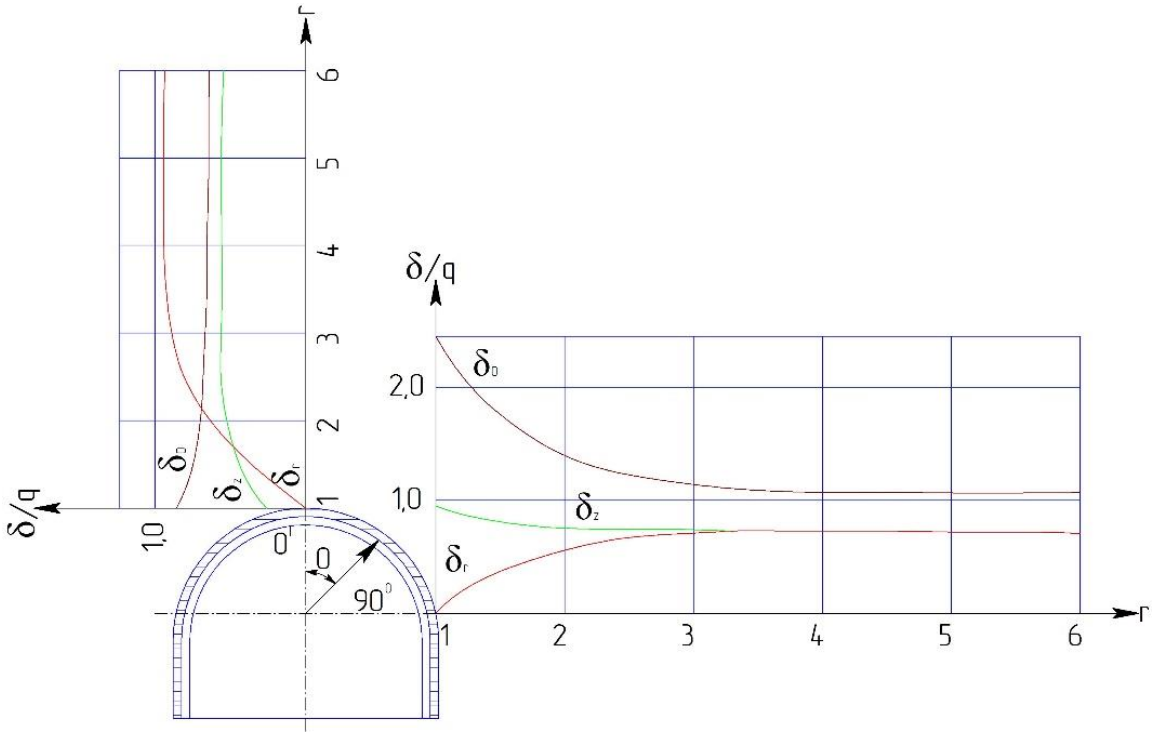

Fig. 2. Stress distribution plots around a horizontal excavation under pre-failure deformation of the rock mass in a non-hydrostatic initial stress field.

3. Results

Solving the problem in terms of additional stresses and assuming the absence of support (p = 0), the boundary conditions can be written as follows [10]**:**

$$\sigma_r = -\left(\frac{1+\lambda}{2} + \frac{1-\lambda}{2}\cos 2\theta\right)q, \qquad \tau_{r\theta} = \frac{1-\lambda}{2} q \sin 2\theta,$$

$$\text{at } r = 1; \ \sigma_r = \sigma_\theta = \tau_{r\theta} \to 0 \to at \to r \to \infty. \tag{8}$$

The components of the additional stresses calculated in this way are expressed as follows [8]:

$$\sigma_r = -q\left[\frac{1+\lambda}{2}\frac{1}{r^2} - \frac{1-\lambda}{2}\left(\frac{3}{r^4} - \frac{4}{r^2}\right)\cos 2\theta\right], \ \sigma_\theta = q\left[\frac{1+\lambda}{2}\frac{1}{r^2} - \frac{1-\lambda}{2}\frac{3}{r^4}\cos 2\theta\right],$$

$$\sigma_z = -q\frac{1-\lambda}{2}\frac{4\mu}{r^2}\cos 2\theta, \qquad \tau_{r\theta} = -q\frac{1-\lambda}{2}\left(\frac{2}{r^2} - \frac{3}{r^4}\right)\sin 2\theta, \tag{9}$$

The components of the initial stresses (7) in the cylindrical coordinate system are expressed as follows:

$$\sigma_r = q\left(\frac{1+\lambda}{2} + \frac{1-\lambda}{2}\cos 2\theta\right), \qquad \sigma_\theta = q\left(\frac{1+\lambda}{2} - \frac{1-\lambda}{2}\cos 2\theta\right),$$

$$\tau_{r\theta} = -\frac{1-\lambda}{2} q \sin 2\theta; \sigma_z = \lambda q. \tag{10}$$

By summing (9) and (10), we obtain the components of the total stresses [9]:

$$\sigma_r = q\left[\frac{1+\lambda}{2}\left(1 - \frac{1}{r^2}\right) + \frac{1-\lambda}{2}\left(1 - \frac{4}{r^2} + \frac{3}{r^4}\right)\cos 2\theta\right]; \qquad \sigma_\theta = q\left[\frac{1+\lambda}{2}\left(1 + \frac{1}{r^2}\right) - \frac{1-\lambda}{2}\left(1 + \frac{3}{r^4}\right)\cos 2\theta\right];$$

$$\sigma_z = q\left[\lambda - \mu\frac{1-\lambda}{2}\frac{4}{r^2}\cos 2\theta\right]; \quad \tau_{r\theta} = -q\frac{1-\lambda}{2}\left(1 + \frac{2}{r^2} - \frac{3}{r^4}\right)\sin 2\theta; \tag{11}$$

It is easily seen that for λ= 1 , the expressions for the stresses correspond to the expressions given above for the axisymmetric case. As an illustration, let us examine the stress state of a homogeneous isotropic rock mass in the vicinity of an unsupported circular excavation (p = 0) with a lateral pressure coefficient λ equal to 0.3 and 0.6.Table 2 presents the values of the total stresses calculated for points along the excavation boundary at angles 0,45 and 90^0. Based on the data in Table 2, stress distribution plots in units of *q* were constructed for λ = 0.6 at points 0 = 00 and 0 = 900 (Fig. 2).

Analyzing the obtained results, it can be seen that when the lateral pressure coefficient λ < 1, changes occur in the stress distribution compared to the case of λ = 1. Specifically, as λ decreases, the tangential stress σ_θ along the horizontal axis of the excavation boundary increases, while along the vertical axis it decreases and, at λ = 1/3, even changes sign, i.e., becomes tensile.

In the presence of technological irregularities along a smooth design boundary of the excavations, the general patterns of stress distribution are preserved at points of maximum curvature (recesses) and minimum curvature (protrusions).

Table 2

r	Stresses in units of q for various radial directions 0									lateral pressure coefficient λ
	σ_r			σ_θ			σ_z			
	0°	45°	90°	0°	45°	90°	0°	45°	90°	
1	0	0	0	-0,1	1,3	2,7	-0,02	0,30	0,62	
2	0,56	0,49	0,42	0,4	0,82	1,23	0,22	0,30	0,38	
4	0,70	0,58	0,46	0,36	0,69	1,04	0,28	0,30	0,32	0,3
6	0,94	0,63	0,32	0,32	0,67	1,02	0,29	0,20	0,31	
10	0,99	0,64	0,30	0,31	0,65	1,01	0,29	0,20	0,30	
1	0	0	0	0,80	1,60	2,10	0,30	0,60	0,88	
2	0,64	0,60	0,56	0,72	1,0	1,38	0,53	0,60	0,08	
4	0,90	0,75	0,62	0,65	0,85	1,05	0,58	0,60	0,62	0,6
6	0,94	0,78	0,61	0,63	0,82	1,03	0,59	0,60	0,61	
10	0,99	0,79	0,60	0,61	0,81	1,01	0,59	0,60	0,60	

To illustrate the proposed solution, we examine the stress state in the vicinity of excavations with different cross-sectional shapes conducted in a homogeneous isotropic rock mass with an initial hydrostatic stress state. The parameters defining the contour shape and form are as follows: for an ellipse - $n=1$, $c_1 = 0{,}14$, for a square $n=3$, $c_1 = 0{,}15$;for a circle - $n = 0$, $c_1 = 0$. The resulting stress values, expressed in units of q , are presented in the form of plots in Fig. 3.

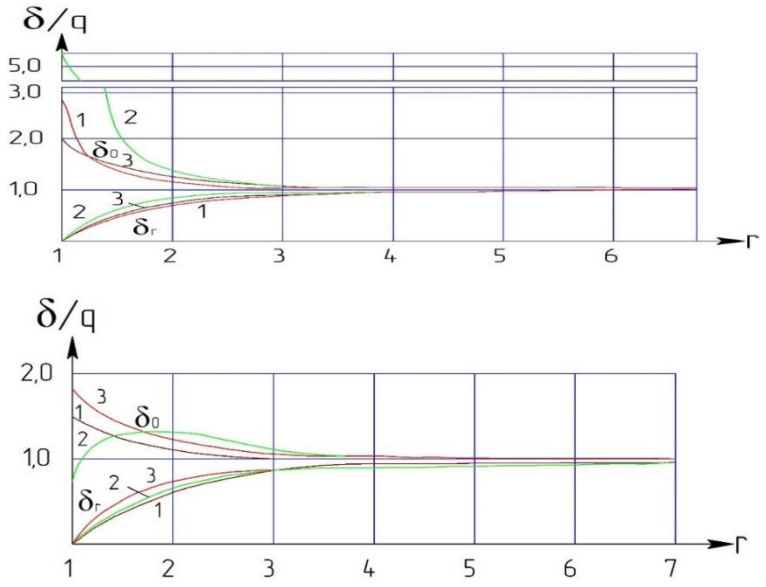

1 – Elliptical contour; 2 – Square contour; 3 – Circular contour

Fig. 3. Stress distribution plots around excavations with different cross-sectional shapes

In Fig. 3.(a), the stress diagrams in the vicinity of the excavations are shown along axes passing through points of maximum contour curvature, whereas in Fig. 3(b) they are shown along axes passing through points of minimum contour curvature.Fig. 4. presents the stress distribution plots of σ_θ along the boundaries of excavations with square and elliptical cross-sections.

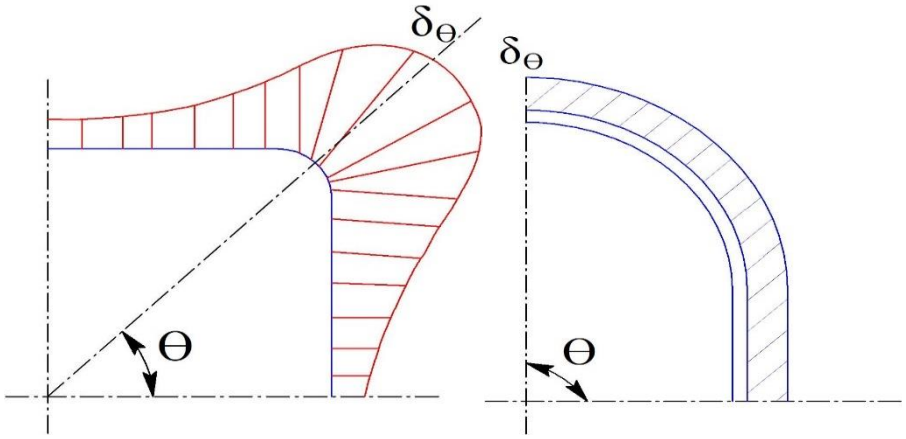

Fig. 4. Stress distribution plots along the boundaries of excavations with square (a) and elliptical (b) cross-sections.

4. Conclusion

Analyzing the stress diagrams, the following conclusions can be drawn. The maximum concentration of σ_θ is located at points of greatest contour curvature (the corner points of a square cross-section, points along the major axis of an elliptical cross-section) and can reach values $\sigma_\theta >> 2q$. In regions of non-circular contours with minimal curvature, $\sigma_\theta < 2q$,i.e., lower than the tangential stresses along the boundary of a circular excavation. As the distance from the boundary increases, the stress concentration rapidly decreases and practically disappears at $r = 5$, regardless of the contour shape, i.e., $\sigma_\theta = \sigma_r = q$.

The presence of technological heterogeneity of explosive origin in the rock mass leads to increased displacements, but at the same time significantly reduces the influence of factors such as a non-hydrostatic initial stress state and the excavation cross-sectional shape. This allows geomechanical models and calculation schemes to be considerably simplified in problems considering the pre-failure deformation stage of rocks. This is due to the fact that the absolute magnitude of displacements along the excavation boundary in rocks at the pre-failure stage is small and does not significantly affect excavation stability.

However, it should be noted that the factors considered can cause unfavorable stress distributions, which in turn may lead to the transition of rocks into the post-failure deformation stage, where geomechanical processes will exhibit qualitatively and quantitatively new behaviors.

References

1. Fadeev, B.A. Finite Element Method in Geomechanics. Moscow: Nedra, 1987. – 236 p.
2. Crouch, S., Starfield, A. Boundary Element Methods in Solid Mechanics. Moscow: Mir, 1987. – 236 p.
3. Nazarov, Z.S., Jiyanov, A.B., Sharipov, L.O. Estimation of Principal Horizontal Stresses Based on Geodynamic Zoning Data of Nearby Analog Deposits // Proceedings of the International Conference on Integrated Innovative Development of the Zarafshan Region: Achievements, Problems, and Prospects. Navoi, Uzbekistan, October 27–28, 2022. Pp. 174–178.
4. Kuznetsov, G.N., Budko, M.N., Filippova, A.A., Shklyarsky, M.F. Study of Rock Pressure Manifestation on Models. Moscow: Ugletekhizdat, 1997. – 283 p.
5. Baklashov, I.V. Deformation and Failure of Rock Masses. Moscow: Nedra, 1988.
6. Nazarov, Z.S., Jiyanov, A.B., Sharipov, L.O., Nazarov, A.Z. Calculation of the Pit Wall Mass Using the Finite Element Method in Midas GTS NX Software // Science and Education in Karakalpakstan. Karakalpakstan, 2023. №1/2(31). Pp. 29–34.

7. Nazarov, Z.S., Jiyanov, A.B., Sharipov, L.O., Sunnatulloev, Sh. Application of Professor D. Lobshire's Geomechanical Classification for In-Depth Zoning of the Amantaytau Mine Board // E3S Web of Conferences, GEOTECH-2023. 417, 01001 (2023). doi:10.1051/e3sconf/202341701001
8. Baklashov, I.V., Kartozia, B.A. Mechanical Processes in Rock Masses. Moscow: Nedra, 1986.
9. Baklashov, I.V., Kartozia, B.A. Mechanics of Underground Structures and Support Constructions. Moscow: Nedra, 1992.
10. Pokrovsky, G.I., Fedorov, I.S. Centrifugal Modeling in Mining. Moscow: Nedra, 1989. – 247 p.